IEEE Access
Multidisciplinary ⋮ Rapid Review ⋮ Open Access Journal

Received 14 October 2023, accepted 31 October 2023, date of publication 6 November 2023, date of current version 14 November 2023.

Digital Object Identifier 10.1109/ACCESS.2023.3330149

RESEARCH ARTICLE

Research on Multi-UAV Formation and Semi-Physical Simulation With Virtual Structure

JIANDONG GUO[1], ZHENGUANG LIU[1], YANGUO SONG[2], CHANGFA YANG[3], AND CHENYU LIANG[4]

[1]College of Automation Engineering, Nanjing University of Aeronautics and Astronautics, Nanjing 210001, China
[2]College of Aerospace Engineering, Nanjing University of Aeronautics and Astronautics, Nanjing 210001, China
[3]Aviation Industry Corporation of China Ltd., Hongdu, Nanchang 330001, China
[4]Nanjing Changkong Technology Company Ltd., Nanjing 210001, China

Corresponding author: Jiandong Guo (bh4rbc@nuaa.edu.cn)

This work was supported by the Fundamental Research Funds for the Central Universities under Grant 56XAC22030.

ABSTRACT In a highly challenging environment, it is difficult to ensure effective information exchange between UAVs due to disruptions and limitations in communication. Aiming at the problem of multiple UAVs' control in this environment, this paper proposes a single-route virtual structure formation method with geometric constraint rules. The position of the virtual leader is continuously updated in real-time along a pre-planned route. By utilizing geometric constraint rules and incorporating the position of the virtual leader, the virtual formation can be accurately calculated. In the straight mode, the formation UAVs generate expected reference points based on the virtual formation. They then calculate the respective reference points of the formation UAVs and use the line-of-sight guidance law to obtain the roll angle command for each UAV, thereby maintaining the formation. In the arc mode, the virtual formation is used as the reference point to calculate the position in real-time, in order to maintain the formation. The roll angle command is obtained based on this position. Upon receiving the formation command, the UAVs update their positions in the virtual formation to complete the formation control individually. Importantly, this method does not require real-time data communication between the UAVs. Nonlinear numerical simulation is conducted to verify the effectiveness of the proposed method in achieving precise formation control. Additionally, a semi-physical simulation platform is built to implement the designed algorithm in engineering. The results further confirm that the algorithm can achieve formation control and effectively reduce the requirements of network radios during task execution.

INDEX TERMS Geometric constraints, virtual structure, UAV formation, semi-physical simulation.

I. INTRODUCTION

In recent years, the unmanned aerial vehicle (UAV) industry has experienced rapid growth, leading to the widespread utilization of UAVs in both military and civilian applications [1]. However, due to the inherent limitations of a single UAV, it is often insufficient to complete complex tasks. As a result, researchers have turned to the cooperation of multiple UAVs to overcome these limitations and accomplish tasks that would be otherwise impossible for a single UAV. The problem of formation control, which involves coordinating the movements of multiple UAVs, is a fundamental and challenging aspect of multi-UAV operations. It has become a prominent area of research in the UAV field [2], [3].

There are several control methods for UAV formation, including the Leader-Follower algorithm [4], [5], [6], Behavior-Based algorithm [7], and Virtual Structure algorithm [8], [9], [10]. Among these, the Leader-Follower algorithm is widely used for UAV formation. In this algorithm, a designated leader guides the formation, while the followers maintain a specific relative distance and angle to the leader, thereby fixing the formation [11]. Based on the Leader-Follower algorithm and nearest neighbor interaction rules, a kind of distributed control algorithm is proposed,

The associate editor coordinating the review of this manuscript and approving it for publication was Xiwang Dong.

which enables all the agents asymptotically coverage to fly with the same velocity and approach the expected formation with their neighbors [12]. On the basis of Leader-Follower algorithm, a control design algorithm based on asymmetric barrier Lyapunov function is presented for Leader-Follower control of Euler-Lagrange systems with unknown parameters and un-modeled dynamics [13]. Literature [14] introduces a cyclic strategy to solve the defects in the Leader-Follower algorithm. The simulation result shows that the designed cyclic strategy is successful in different scenarios and ensures the stability of the UAV formation during the substitution of the leader. According to the needs of the task, the Behavior-Based algorithm assigns the appropriate behavior to the UAV, and obtains the formation control input by means of weighted average. Aiming at the collision problem between UAVs, literature [15] designs a formation control method using the behavior-based algorithm, and divides the formation behavior into four behaviors: aggregation, separation, speed consistency and obstacle avoidance. In the obstacle avoidance behavior, speed obstacle method and potential field method are introduced. Using only the relative information between UAVs and its adjacent UAVs and obstacles, Lee et al. propose a decentralized behavior-based formation control algorithm for UAV formation considering obstacles avoidance [16]. The Virtual Structure algorithm sets a virtual geometric center in the formation, which is used by the rest of the UAVs as a reference to obtain the corresponding expected position. By integrating virtual structure concept with differential flatness-based feedback control, Zhou et al. present a method for controlling quadrotors formation to preform agile interleaved maneuvers while holding a fixed relative formation, or transitioning between different formations [17]. In literature [18], aiming at the problem that there exist local minima in the collision avoidance for the UAVs using artificial potential field, a composite vector artificial potential field in three-dimensional space is proposed based on the Virtual Structure and the Leader-Follower algorithm, which can avoid the obstacle and track the moving target effectively. Rabelo et al. present a solution based on Virtual Structure to the problem that caused by the challenge of landing an UAV on static or mobile platforms. Based on the theory of Lyapunov, the effectiveness of this method is checked through experimental results [19].

The applications of multi-UAV formations include trajectory optimization [20], [21], mission planning [22], [23], [24], etc. In literature [25], in order to research intelligent multi-UAV reconnaissance mission planning and online re-planning algorithm under various constraints in mission areas, a reconnaissance mission planning and re-planning system is established. Yu et al. develop an improved genetic algorithm with a novel chromosome encoding format, which can determine the number of attacks on a given target based on the expectations obtained, rather than being predetermined [26]. In order to solve the cooperative mission assignment for heterogeneous UAVs, an improved multi-objective genetic algorithm, which incorporates a natural chromosome encoding format and specially designed genetic operators, is developed [27]. To deal with the issue of trajectory planning problem of autonomous dispatch on flight deck, a search-resampling-optimization framework is proposed, which can be easily extended to the trajectory planning problem in other fields [28]. Literature [29] proposes an optimal control-based method with efficient warm-start to solve the trajectory planning problem for fixed-wing UAV formations. Through numerical simulations at various complexity levels, the robustness and efficiency of the proposed planner is verified. To address the challenge of real-time trajectory planning during the transformation process from triangular formation to circular formation under different states, a trajectory planning method integrating Dubins trajectory and particle swarm optimization algorithm is proposed [30].

In order to solve the problem of multi-UAV formation in scenarios with limited communication, Ge et al. propose a dynamic event-triggered communication mechanism to schedule inter-agent communication, effectively reducing unnecessary data exchanges among agents [31]. Based on ultraviolet light, Walter et al. present a novel onboard relative localization method, which enables real-time control of a Leader-Follower formation of multirotor UAVs without the need for communication [32]. However, this method is not suitable for situations where the distance between UAV formations is large. Liu et al. tackle the problem of robust visual servoing formation tracking for quadrotor UAVs by designating a UAV captured using onboard cameras as the leader and implementing a switching topology strategy to ensure the cooperative work of the quadrotor formation [33]. Similarly, this method is not suitable for situations where the UAV is located at a significant distance.

In this paper, we propose a method for UAV formation control by combining the Virtual Structure algorithm based on geometric constraint rules with the line-of-sight guidance law [34]. The method involves selecting a formation shape and determining the expected reference points of the virtual formation. The reference points of the actual formation are then calculated based on geometric constraint rules. Next, the line-of-sight guidance law is used to solve the attitude angle and speed commands for each UAV in the formation, enabling the UAV formation to track the desired reference points. To validate the effectiveness of the proposed formation control method, numerical and semi-physical simulations are conducted [35], [36], [37]. The simulation results demonstrate that the method, which is easily implementable in engineering, can accurately track the target route. Compared with other current algorithms, this algorithm proposed in this paper can solve the formation problem in a challenging environment.

II. FORMATION GEOMETRY CONSTRAINT RULES

A. FORMATION STRUCTURE DESIGN

As indicates in Fig.1, in order to verify the efficiency of the method designed in this paper, the formation control

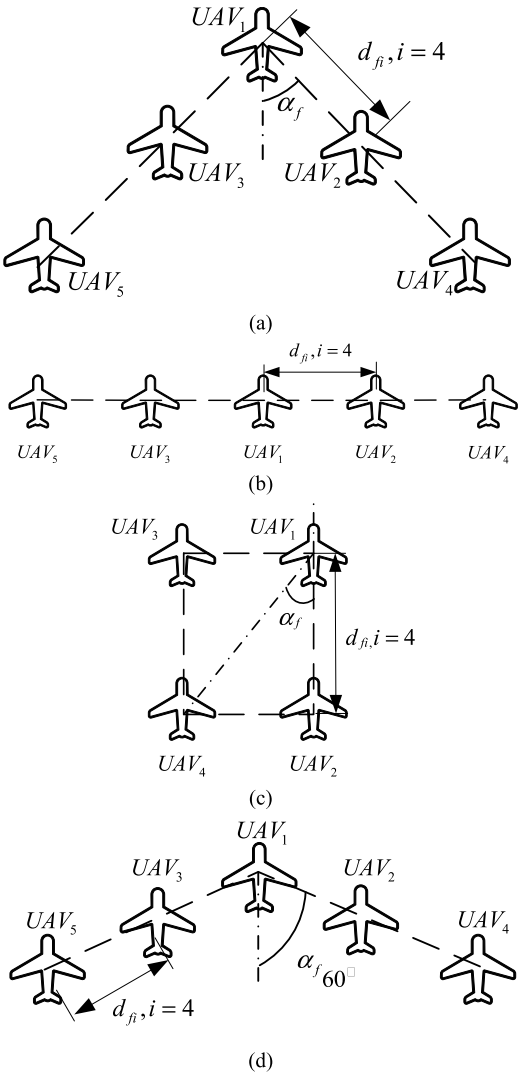

FIGURE 1. Schematic diagram of typical formation shapes. (a) "V" formation shape; (b) Line-shaped formation; (c) Rectangular formation; (d) Down-120° formation.

algorithm in this paper adopts the four formation shapes. The angle at the top of the "V" is $2\alpha_f$ (when the formation UAV is on the right side of UAV_1, α_f is positive, conversely, α_f is negative), and the distance between adjacent UAVs is d_f [38].

B. VIRTUAL FORMATION DESIGN

As depicted in Fig.2, a virtual formation $P, P = PV_i$ $(i = 1, 2, 3 \cdots I)$ is defined as a reflection of the actual formation, where, I denotes the number of virtual UAVs, and PV_i is the virtual UAV corresponding to the *ith* formation UAV. PV_1 is selected as the virtual leader, which flies along straight routes $WP_1 - WP_2$ and $WP_2 - WP_3$ at a constant speed V_0.

Based on the geometric constraints of the virtual formation P and formation shape, the specific position of each virtual UAV within the formation P is calculated. The position of

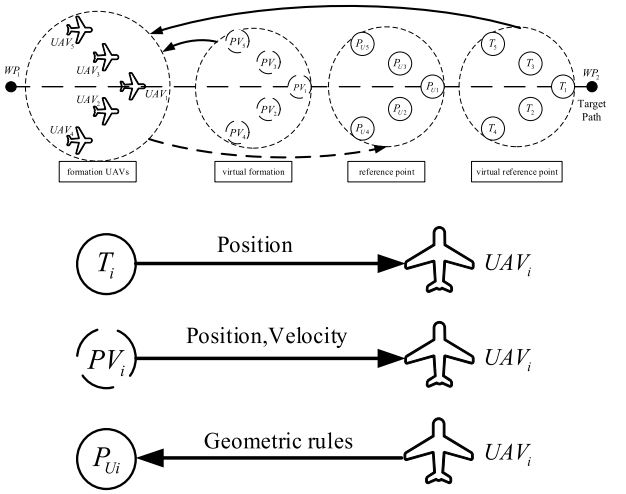

FIGURE 2. Multi-UAV formation topological structure.

PV_2 is solved using (1) (similarly, the positions of other virtual UAVs can be obtained in the same way):

$$\begin{cases} PV_{2N} = PV_{1N} - d_{f2}\cos\left(\psi_{seg1} - \alpha_{f2}\right) \\ PV_{2E} = PV_{1E} - d_{f2}\cos\left(\psi_{seg1} - \alpha_{f2}\right) \\ \psi_{seg1} = \arctan(\dfrac{WP_{2,E} - WP_{1,E}}{WP_{2,N} - WP_{1,N}}) \in [-\pi, \pi], \end{cases} \tag{1}$$

where, PV_{1N}, PV_{1E} and PV_{2N}, PV_{2E} are respectively denote the components of PV_1 and PV_2 in the N, E(N is in the north direction and E is in the east direction) direction.

As illustrated in Fig.3, ψ_{seg1} is the angle between the straight route and the north direction. d_{f2} is the distance between PV_1 and PV_2, and the include angle is α_{f2}.

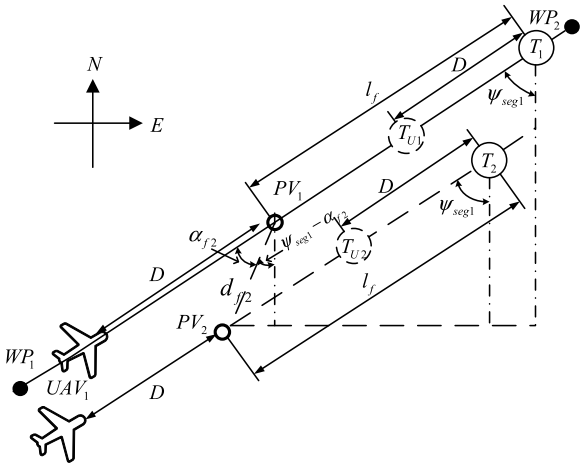

FIGURE 3. Schematic diagram of formation in straight mode.

C. DESIGN OF EXPECTED REFERENCE POINTS FOR FORMATION

Based on the virtual formation and its position described in Section II-B, along with the tracking distance l_f of the virtual

leader relative to the expected reference point T_i, the expected reference point T_i of the virtual formation is determined. The actual formation receives the virtual formation's position, velocity information and point coordinates of T_i in real time to calculate the desired reference point T_{Ui}.

The expected reference points T_1 (T_{1N}, T_{1E}) and T_2 (T_{2N}, T_{2E}) of the virtual formation are determined by:

$$\begin{cases} T_{1N} = PV_{1N} + l_f \cdot sgn\left(WP_{2,N} - WP_{1,N}\right)\cos\psi_{seg1} \\ T_{1E} = PV_{1E} + l_f \cdot sgn\left(WP_{2,N} - WP_{1,N}\right)\sin\psi_{seg1} \\ T_{2N} = PV_{2N} + l_f \cdot sgn\left(WP_{2,N} - WP_{1,N}\right)\cos\psi_{seg1} \\ T_{2E} = PV_{2E} + l_f \cdot sgn\left(WP_{2,N} - WP_{1,N}\right)\sin\psi_{seg1}, \end{cases} \tag{2}$$

where, sgn () is the sign function.

The expected reference points T_i of other UAVs in the virtual formation can be solved similarly. By considering the expected distance D between the virtual formation and the actual formation, the expected reference points T_{U1} (T_{U1N}, T_{U1E}) and T_{U2} (T_{U2N}, T_{U2E}) for UAV_1 and UAV_2 can be further obtained as:

$$\begin{cases} T_{U1N} = T_{1N} - D \cdot sgn\left(WP_{2,N} - WP_{1,N}\right)\cos\psi_{seg1} \\ T_{U1E} = T_{1E} - D \cdot sgn\left(WP_{2,N} - WP_{1,N}\right)\sin\psi_{seg1} \\ T_{U2N} = T_{2N} - D \cdot sgn\left(WP_{2,N} - WP_{1,N}\right)\cos\psi_{seg1} \\ T_{U2E} = T_{2E} - D \cdot sgn\left(WP_{2,N} - WP_{1,N}\right)\sin\psi_{seg1} \end{cases} \tag{3}$$

The expected reference points of the rest of the UAVs in the formation can be solved using (3) to track the route designed in this paper.

III. FORMATION ALGORITHM DESIGN

A. LATERAL POSITION CONTROL IN STRAIGHT MODE

During the flight of the formation along the straight route $WP_1 - WP_2$, the lateral position and roll angle command of the formation UAVs are calculated by substituting the ground speed V_g, track angle Ω and the angle between UAV and the expected reference point T_{Ui} into the line-of-sight guidance law. Now let's take UAV_1 as an example.

The position of UAV_1 is U_1 (U_{1N}, U_{1E}), and the component of flight speed in the NED coordinate system is (V_{1N}, V_{1E}). The ground speed V_{g1} and track angle Ω_1 can be expressed as:

$$\begin{cases} V_{g1} = \sqrt{(V_{1E})^2 + (V_{1N})^2} \\ \Omega_1 = \arctan\left(V_{1E}, V_{1N}\right). \end{cases} \tag{4}$$

The angle β_{f1} between the line connecting UAV_1 and its expected reference point T_{U1} (T_{U1N}, T_{U1E}) and N direction of coordinate system is:

$$\beta_{f1} = \arctan\left(\left(T_{U1E} - U_{1E}\right), \left(T_{U1N} - U_{1N}\right)\right). \tag{5}$$

Combined with the line-of-sight guidance law, the desired roll angle ϕ_1 can be given by:

$$\phi_1 = \frac{2V_{g1}^2 \sin\left(\beta_{f1} - \Omega_1\right)}{l_f' g}, \tag{6}$$

where, g denotes the acceleration of gravity, and l_f' is the length of UAV_1 tracking T_{U1}.

In the same manner, the expected roll angle of other UAVs can also be given by:

$$\phi_i = \frac{2V_{gi}^2 \sin\left(\beta_{fi} - \Omega_i\right)}{l_f' g}. \tag{7}$$

B. LATERAL POSITION CONTROL IN ARC MODE

As shown in Fig.4, when the expected reference point T_1 of the virtual leader reaches the endpoint WP_2 of the first section of the route, it enters the arc mode. At this time, the virtual leader is located at the mode entry point. By utilizing the geometric relationship, the coordinates (A_N, A_E) of A can be obtained, and similarly, the coordinates of the modal washout point B (B_N, B_E) can also be obtained as:

$$\begin{pmatrix} A_N \\ A_E \\ B_N \\ B_E \end{pmatrix} = \begin{pmatrix} WP_{2,N} \\ WP_{2,E} \\ WP_{2,N} \\ WP_{2,E} \end{pmatrix} + l_f \begin{pmatrix} -sgn\left(WP_{2,N} - WP_{1,N}\right)\cos\psi_{seg1} \\ -sgn\left(WP_{2,N} - WP_{1,N}\right)\sin\psi_{seg1} \\ sgn\left(WP_{3,N} - WP_{2,N}\right)\cos\psi_{seg2} \\ sgn\left(WP_{3,N} - WP_{2,N}\right)\sin\psi_{seg2} \end{pmatrix}, \tag{8}$$

where, ψ_{seg1}, ψ_{seg2} represent the angles between route $WP_1 - WP_2$, $WP_2 - WP_3$ and N respectively.

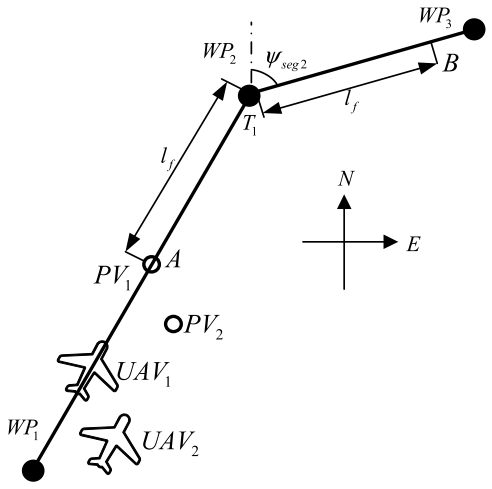

FIGURE 4. Arc mode judgment conditions.

The virtual leader flies along the arc route in this mode, as shown in Fig.5, and its position (PV_{1N}, PV_{1E}) is obtained

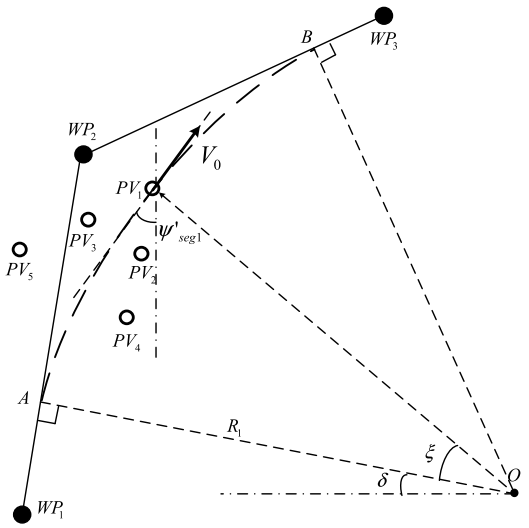

FIGURE 5. Formation control algorithm in the arc mode.

by the geometric constraint rules of the arc:

$$\begin{cases} PV_{1N} = O_N + R_1 \sin(\delta + \xi) \\ PV_{1E} = O_E - R_1 \cos(\delta + \xi), \end{cases} \tag{9}$$

where, (O_N, O_E) is the inscribed circle center of the route $WP_1 - WP_2$, $WP_2 - WP_3$, R_1 is the radius of the inscribed circle corresponding to the virtual leader, and δ is the angle between the line connecting the virtual leader at point A and the center of the circle and the E direction, which can be expressed as:

$$\delta = \arctan\left((A_N - O_N), (A_N - O_N)\right). \tag{10}$$

In the arc mode stage, the positions of the other virtual UAVs PV_i in the virtual formation can still be obtained by (1) and (2).

The central angle ξ of the arc route of the virtual leader can be calculated from the speed V_0 of the virtual leader and the flight time t of the arc mode, which is obtained as:

$$\begin{cases} \omega = \dfrac{V_0}{R_1} \\ \xi = \omega t \end{cases} \tag{11}$$

The angle ψ'_{seg1} between the arc tangent of the inscribed circle between the route $WP_1 - WP_2$, $WP_2 - WP_3$ and the N direction is:

$$\psi'_{seg1} = \delta + \xi. \tag{12}$$

In this mode, the PV_i will be used as the expected reference point. According to (7), the roll angle command required by each UAV can be obtained.

In this paper, the following conditions are used as the washout flags of the arc mode.

1) Condition 1 is:

$$\arccos\left(\frac{\overrightarrow{OPV_1} \bullet \overrightarrow{WP_2WP_3}}{\left|\overrightarrow{OPV_1}\right| \left|\overrightarrow{WP_2WP_3}\right|}\right) \le 0.01, \tag{13}$$

where, $\overrightarrow{OPV_1}$ is the vector from the center O of the circle to PV_1. As shown in Fig.6, $\left|\overrightarrow{OPV_1}\right|$ is the modulus value of $\overrightarrow{OPV_1}$. $\overrightarrow{WP_2WP_3}$ is the vector from WP_2 to WP_3, and its modulus value is $\left|\overrightarrow{WP_2WP_3}\right|$.

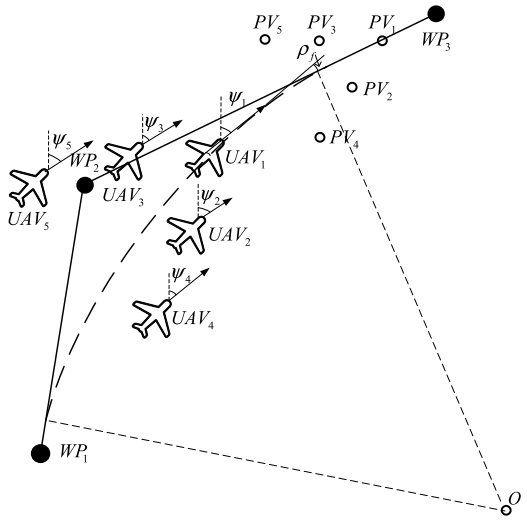

FIGURE 6. Conditions for judging washout in arc mode.

2) Condition 2 is:

$$\left|\psi_i - \psi_{seg2}\right| < \rho_f, \tag{14}$$

where, ρ_f is the washing out threshold, and ψ_i is the track angle of the *ith* formation UAV.

To determine whether the arc mode is washed out, the following two steps are used:

Step1: According to condition 1, it is determined whether the virtual leader has completed the arc mode;

Step2: After condition 1 is met, the switch of the expected reference point from PV_i to T_{Ui} is judged according to condition 2. When the track angle of each formation UAV satisfies condition 2, it indicates that the arc mode is washed out.

C. LONGITUDINAL FORMATION MAINTAIN

To account for biases that may arise due to external disturbances during the formation's tracking the expected reference points, this paper proposed a longitudinal position controller and takes the following bias between the actual and virtual formation as the input of the controller

In order to mitigate the longitudinal position bias of each UAV caused by the different radii when flying in a circular arc, two modes, the straight mode and the arc mode, are designed respectively.

1) STRAIGHT MODE CONTROL ALGORITHM

As indicates in Fig.7, the actual distance D_i between UAV_i (U_{iE}, U_{iN}) and the virtual UAV PV_i (PV_{iN}, PV_{iE}) is

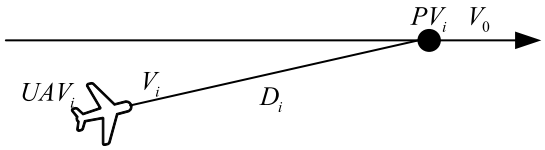

FIGURE 7. Straight mode following bias.

denoted as:

$$D_i = \sqrt{(U_{iE} - PV_{iE})^2 + (U_{iN} - PV_{iN})^2}. \tag{15}$$

Then, the distance following bias e_{Di} of UAV_i can be calculated by:

$$e_{Di} = D_i - D. \tag{16}$$

In this mode, the speed of the virtual formation is consistent with the speed V_0 of the virtual leader, and the speed error between virtual leader and UAV_i is given by:

$$e_{Vi} = V_0 - V_i, \tag{17}$$

where, V_i is the flight speed of formation UAV.

2) ARC MODE CONTROL ALGORITHM

In the arc mode, the distance following bias e_{Di} is the same as that in the straight mode.

As depicted in Fig.8, when the formation UAVs turn along the arc route, the speed bias is calculated according to the flight radius R_i and V_0.

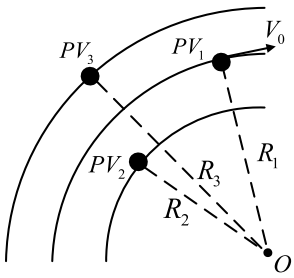

FIGURE 8. Different flight radius in the arc mode.

The difference ΔR between the radius R_i of the arc and the radius R_1 of the inscribed circle of the virtual leader is denoted as:

$$\Delta R = d_{fi} \sin \alpha_{fi}. \tag{18}$$

The value of R_i is divided into two situations. When UAVs turn left along the flight direction and PV_i is on the left side of PV_1, R_i is $R_1 - \Delta R$, on the contrary, R_i is $R_1 + \Delta R$.

The speed bias e_{Vi} of each formation UAV is obtained as:

$$\begin{cases} V_{icmd} = V_0 \left(R_i / R_1\right) \\ e_{Vi} = V_i - V_{icmd}, \end{cases} \tag{19}$$

where, V_{icmd} is the expected speed of the formation UAV.

According to the following bias e_{Di}, e_{Vi} of straight mode and arc mode, the input e_x of the longitudinal position keeping controller is determined by the following formula:

$$e_x = k_D e_{Di} + k_V e_{Vi}. \tag{20}$$

The longitudinal position keeping controller is designed as:

$$\delta_T = k_{px} e_x + k_{ix} \int e_x dt + k_{dx} \dot{e}_x, \tag{21}$$

where, δ_T is the throttle output, and k_D, k_V, k_{px}, k_{dx} are control law parameters used to realize the longitudinal position control in formation flight.

Note: The formation control method proposed in this paper can be combined with inter-vehicle collision avoidance methods to prevent collisions between UAVs within the formation during flight. For instance, in practical applications, the design method in this paper can be combined with the anti-collision strategy mentioned in literature [39], using the positional information between adjacent UAVs obtained by onboard sensors. A safety threshold can be set, and when the safety distance between adjacent UAVs is less than this threshold, the anti-collision strategy mentioned in the literature can be executed. Otherwise, the control method designed in this paper can be implemented.

IV. NUMERICAL SIMULATION VERIFICATION

To validate the rationality of the formation control method designed in this paper, a numerical simulation is conducted using five aircrafts. The formation adopts the typical "V" shape depicted in Fig.1(a), where $d_f = 200$ m, $2\alpha_f = 90°$. The tracking distance l_f of the virtual leader relative to the expected reference point T_i is set to 150m, and the desired distance D between the virtual and actual UAV formation is 150m. Each UAV flies from the initial position (0, 0, −200), (−110, 110, −200), (−100, −120, −200), (−200, 200, −200), (−220, −210, −200), and flies along the route $WP_1 - WP_2$ and $WP_2 - WP_3$ at an initial speed of 40m/s. The information of waypoint position is provided in TABLE 1.

TABLE 1. Waypoint coordinate.

Waypoint	NED coordinate(m)
WP_1	(500, 0, -200)
WP_2	(3000, 0, -200)
WP_3	(4500, 1500, -200)

The simulation results of the UAV formation tracking the predetermined route are presented in Fig.9.

The full trajectory of the formation flight process is depicted in Fig.9(a). From the simulation results, it can be observed that in 0-17 s, due to the random distribution of the initial position of the UAVs, each UAV adjusts its flight

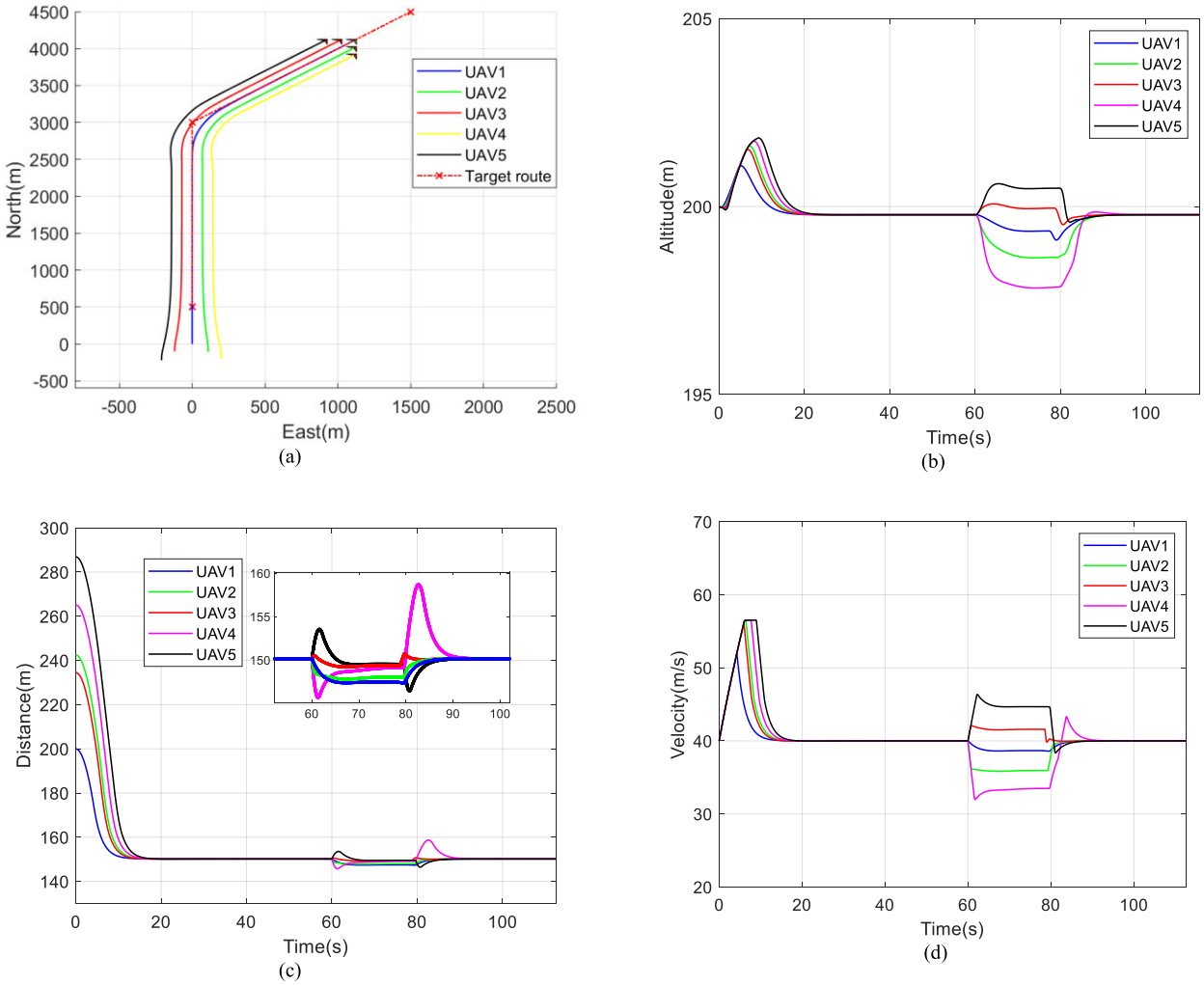

FIGURE 9. Numerical simulation results. (a) Formation flight trajectory; (b) Formation UAV altitude; (c) Relative distance between the UAV and the reference point; (d) Velocity of formation UAVs.

speed and attitude angle to gradually form the expected formation while tracking the expected reference points. During this position adjustment phase, because of the changes in speed and attitude, the height of each UAV fluctuates with an amplitude of less than 1.8m, as shown in Fig.9(b). In 17-60 s, the formation has reached the expected configuration, and each UAV enters a stable flight stage with constant speed and altitude, and a stable distance of 150m from the desired reference points, as shown in Fig.9(c). In 60-95 s, the formation UAVs switch routes. In this stage, the arc route is adopted to facilitate a smooth transition, and the reference points of the UAVs will be switched from T_{Ui} to PV_i. The switching of the reference points leads to changes in the tracking distance between the UAVs and the reference points. Each UAV flies under the guidance of PV_i to maintain the formation. As shown in Fig.9(d), the flight speed of the UAV changes by ± 7 m/s to accommodate the different flight radii in the arc mode. In 95-113 s, the arc mode flight is completed. At this time, the expected reference points of the formation are switched from PV_i to T_{Ui} to adjust the speed and attitude for the subsequent straight mode.

The numerical simulations demonstrate that the formation control algorithm designed in this paper can accurately track the designed route and maintain the predetermined formation. However, it should be noted that the bias in the arc mode may become more evident in subsequent semi-physical simulations.

V. SEMI-PHYSICAL SIMULATION VERIFICATION

A. CONSTRUCTION OF SIMULATION PLATFORM

The multi-UAV formation algorithm designed in this paper has been implemented in engineering. In this section, a semi-physical simulation platform is built to verify the correctness of the algorithm and its practicability. This semi-physical simulation hardware platform consists of four flight control computers, four PC hosts and serial communication cables,

as shown in Fig.10. PC1, PC2 and PC3 are mainly used to run ground control station software (GCS), semi-physical simulation software (H-Sim) and flight simulation software (FG-UAVx, x = 1,2,3), which share the same configuration environment. PC4 runs ground control station software (GCS) and flight model software to display the formation of the virtual leader and three formation UAVs. The flight control system (FCSx, x = 1,2,3) represents the formation of three UAVs. The information exchange computer FCS packages and transmits the information of the three formation UAVs to PC4. Taking UAV1 as an example, the H-Sim running on PC1 and FG-UAV1 perform data interaction through UDP. H-Sim sends the state parameters of UAV1 to FCS1 via COM2 for closed-loop control. Simultaneously, the control command calculated by FCS1 is sent to FG-UAV1 to control the flight of the UAV. FCS1 performs route binding, flight track display and storage, etc. through COM1 and GCS in PC1. FCS1 sends FG-UAV1 formation flight data to FCS through COM3. The other two UAVs communicate in the similar method. The FCS collects the data of the three formation UAVs through COM1, COM2 and COM3 respectively, and then sends them to the GCS of PC4 via COM4 for comprehensive display and data storage of the formation UAVs.

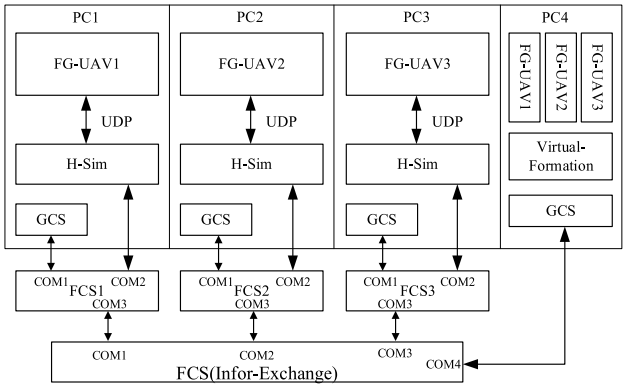

FIGURE 10. Structure diagram of semi-physical simulation platform.

The core of the flight controller of the formation UAV adopts the ARM-CortexM7 architecture, of which the main frequency is 400M Hz. The peripheral interface mainly includes 12 channels of PWM signals, 7 channels of serial ports (2 channels of RS232, 4 channels of TTL, 1 channel of RS422), 4 channels of AD sampling, 1 channel of CAN1 bus, I2C, SPI serial bus and SBus to meet the needs of UAV control. Fig.11 illustrates the flight controller unit.

B. SIMULATION ENVIRONMENT SETUP

Using the built-in model Cessna182 of FlightGear as the formation UAV, the semi-physical simulation experiment of the flight control machine hardware in the loop is carried out. The No. 24 runway of Nanjing Lukou Airport is set as the take-off site, and the formation route adopts WGS84 coordinate system. Use the formation shapes described in Fig.1 to conduct

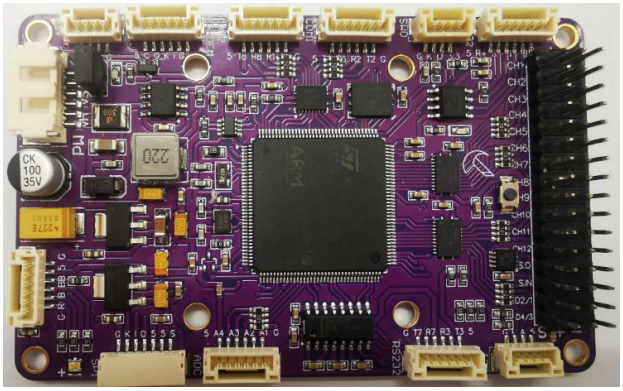

FIGURE 11. The flight controller unit.

semi-physical simulations, where, the angle $2\alpha_f$ in the "V" formation is 90°, and the d_f in Fig.1(a), (b), (c) and (d) is $141m$, $100m$, $115m$ and $115m$, respectively. The expected distance between the virtual and the actual formation is 150 m. The FlightGear flight simulator outputs the flight data of the formation at 60 Hz, the attitude control loop calculation frequency of the FCS is 100Hz, and the formation control frequency is 20 Hz.

The formation route adopts a quadrilateral route with a length of 10.6 Km and a width of 6.6 Km. The set altitude of the virtual formation is 200 m, the cruise speed is 53 m/s, and the turning radius of each UAV is 1.0 Km. The simulation interface of formation process is shown in Fig.12.

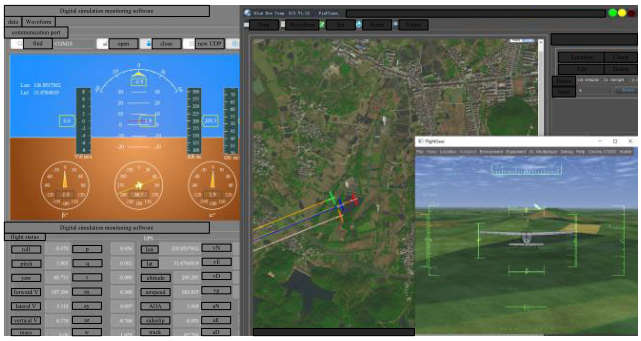

FIGURE 12. Semi-physical simulation interface of multi-UAV formation.

C. SIMULATION DATA ANALYSIS

In the initial stage of the simulation, the same route data is bound for each flight controller through the ground measurement and control software. In this V-shaped simulation example, UAV1 is set as the leader of the "V" formation, with UAV2 positioned at the right rear of UAV1 and UAV3 at the left rear of UAV1. Based on the geometric relationship of formation UAVs, it can be obtained that UAV2 and UAV3 are distributed symmetrically on both sides of the flight route, with the lateral distance of 100m and the longitudinal distance of 150m from the virtual formation. Fig.13 illustrates the flight trajectory of the formation UAVs. Following the program segment design process, the UAVs climb to a certain

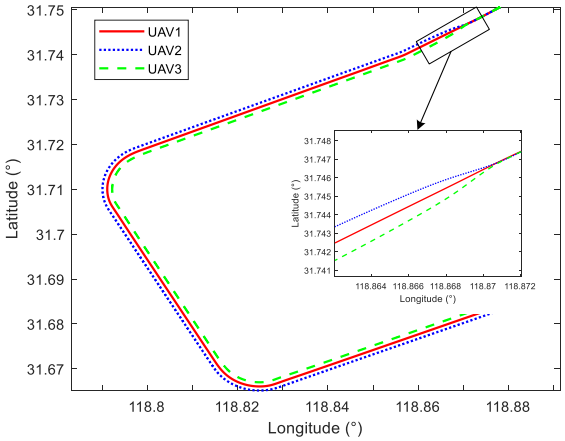

FIGURE 13. Flight trajectory in semi-physical simulation.

altitude and enter the temporary route, guiding them towards the first waypoint It can be observed from the partially enlarged diagram in Fig.13 that UAV2 and UAV3 perform lateral distance adjustment. Once UAV1 approaches the first waypoint of the preset route, the formation command is triggered by the ground. At this point, the virtual formation starts to run, to be tracked by the three UAVs.

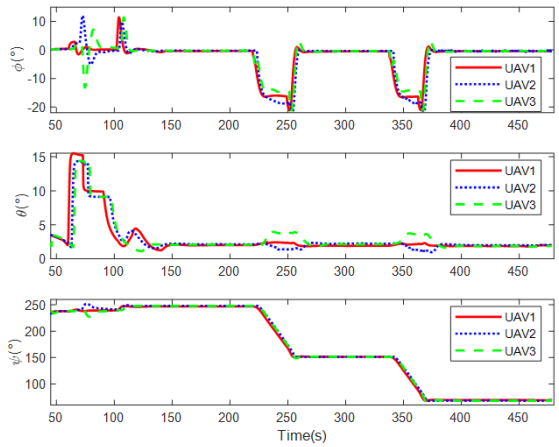

FIGURE 14. Attitude angle response of the formation.

Fig.14 depicts the attitude angle response curve of three UAVs in formation. When the simulation time reaches 60 s, the ground speed of the aircraft reaches 40 m/s to start climbing with the pitch angle of 15°. As the flight altitude reaches 50 m, the UAVs enter the temporary route. Due to the lateral adjustment of UAV2 and UAV3 to a distance of 100 m, there is a significant change in roll angle. As the height of UAVs increases, the pitch angle gradually decreases to achieve a closed-loop control at the height of 200 m. When the flight time reaches about 103 s, the formation command is triggered, and the three UAVs start to track the virtual formation. Since the formation have just entered the formation stage, the longitudinal distance bias between the actual and the virtual formation is large. In order to minimize this bias, the UAVs start to accelerate. It can be seen from Fig.16 that at 150 s into the simulation, the formation distance reaches designed 150 m in the longitudinal direction, and the lateral distance is maintained at 100 m. At this time, the formation is successfully formed.

When the simulation time reaches 220 s, the formation initiates the first left-turn flight. As shown in Fig.14, the roll angle reaches a maximum of approximately 21°, and the heading angle is adjusted from 248° to 152° to enter the second straight segment flight. During the arc mode, UAV2, being on the outside of the formation, has a larger turning radius compared to UAV1. In order to maintain the formation, UAV1 accelerates to a maximum of 59 m/s, while UAV2 accelerates to a maximum of 45 m/s, the speed change curve is shown in Fig.15. In the arc mode, the altitude control accuracy is excellent. However, due to the change in speed, UAV3 experiences a descent of approximately 7 m, while UAV2 climbs by 2 m.

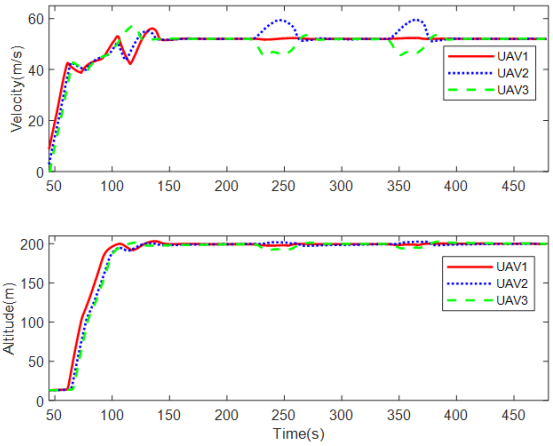

FIGURE 15. Ground speed and altitude response of the formation.

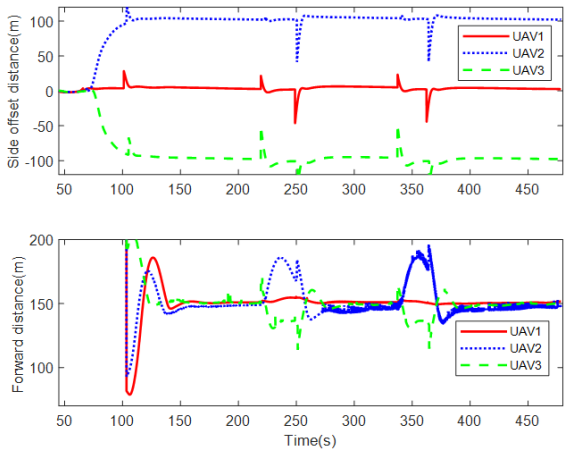

FIGURE 16. Lateral and longitudinal distances of the formation.

It can be seen from Fig.16 that the formation UAVs maintain a lateral position of approximately 100 m in the straight mode and the arc mode, with a control bias of less than 4 m. The peak value in this figure is primarily due to the need for

the fixed-wing aircraft to change the route in advance when transitioning between the straight mode and the arc mode. Therefore, it is not used as an assessment indicator for the formation. Additionally, it can be observed that the control accuracy of the longitudinal distance of the three UAVs is better in the straight mode, with a control bias of less than 8 m. In the arc mode, the control accuracy of the longitudinal formation is slightly reduced due to the acceleration and deceleration of the outside and inside UAVs of the formation. However, the formation can quickly restore its accuracy after entering the straight mode.

The remaining simulations adopt the same flight route as the "V" formation, and the simulation results are shown in Fig.17, Fig.18 and Fig.19.

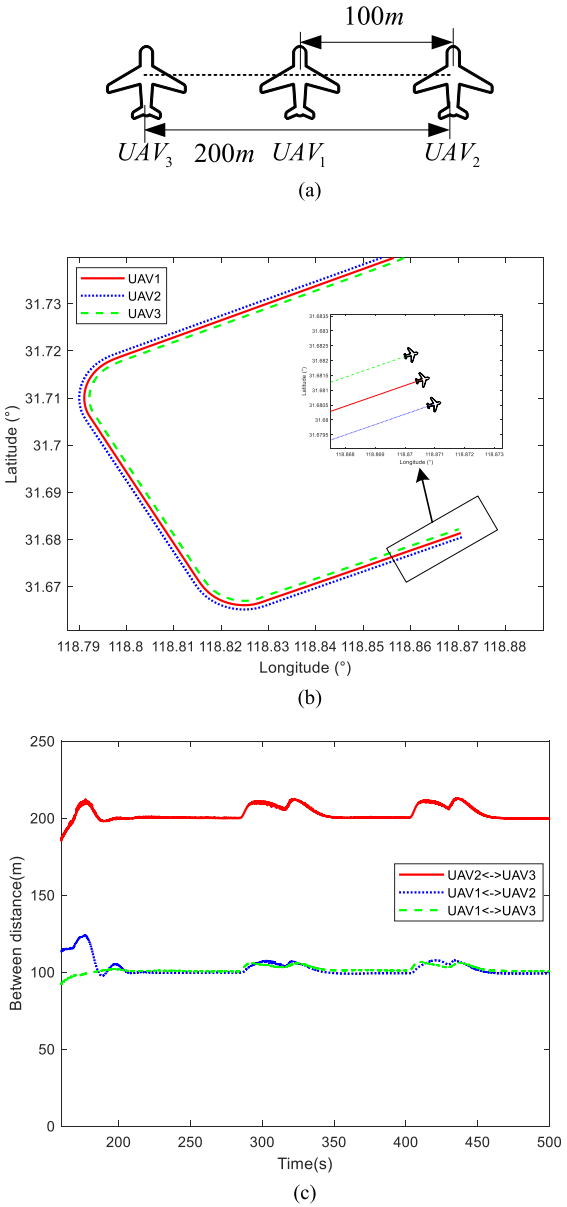

FIGURE 17. Line-shaped formation maintenance effects. (a) Formation data; (b) Flight route of line-shaped formation; (c) Distance between UAVs while flying.

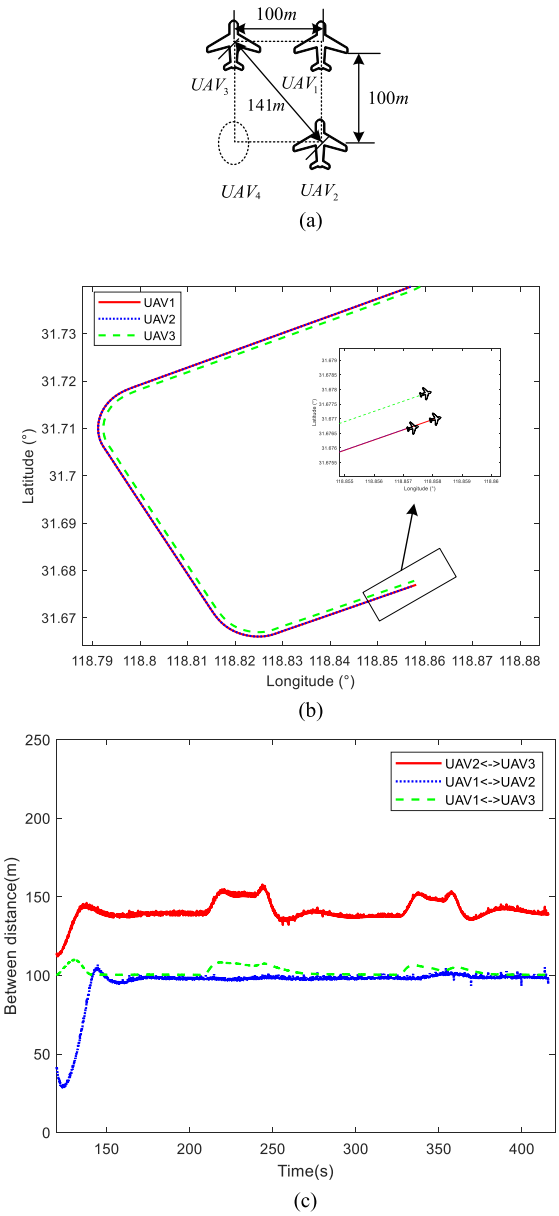

FIGURE 18. Rectangular formation maintenance effects. (a) Formation data; (b) Flight route of partial rectangular formation; (c) Distance between UAVs while flying.

As depicted in Fig.17(a), in the line-shaped formation, the distance between adjacent UAVs is 100 m. The formation maintenance effects are illustrated in Fig.17(b) and (c).

From Fig.17(b), it can be observed that the three UAVs can maintain the pre-defined line-shaped formation effectively. In Fig.17(c), the distance of adjacent UAVs is kept at 100 m with a maximum error of 1.25 m when flying in straight mode, and the distance between UAV2 and UAV3 is maintained at 200 m with a maximum error of 1.48 m. Due to the turning of the formation, UAV3 needs to slow down and UAV2 needs to accelerate, causing the distance between the aircraft to fluctuate.

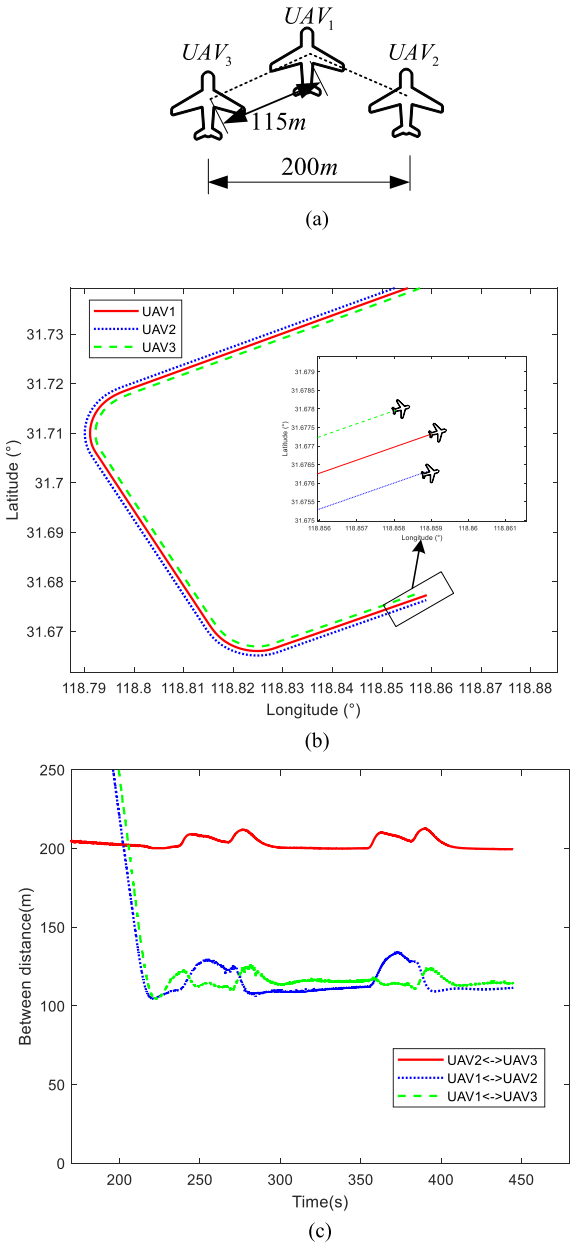

FIGURE 19. Down-120° formation maintenance effects. (a) Formation data; (b) Flight route of down-120° formation; (c) Distance between UAVs while flying.

In Fig.18(a), a partial rectangular formation is also designed, in which the preset distance between UAV1 and UAV2 is 100 m and the distance between UAV2 and UAV3 is 141 m.

As shown in Fig.18(b) and Fig.18(c), three UAVs maintain their partial rectangular formation well. In the first straight mode, the distance between adjacent UAVs is maintained at 100 m with a maximum error of 0.56 m. During the next straight mode, from 268 s to 328 s, the distance error between adjacent UAVs is initially large due to the previous arc mode, but gradually becomes smaller. And the distance between UAV2 and UAV3 maintains at 141 m with a maximum error of 3.84 m in straight mode.

A semi-physical simulation experiment has also been conducted for the down-120° formation in Fig.19(a). The distance between the UAV1 and UAV2 is 115m and the distance between UAV2 and UAV3 is 200 m.

In the straight mode, the distance between the UAVs is close to the preset value, and in the arc mode, due to the different turning radii, the bias increases. After switching to straight mode, the distance between the UAVs gradually converges to the expected value.

After conducting semi-physical simulation experiments of four formations, it has been observed that the method described in this paper is capable of maintaining a stable formation during flight, particularly in the straight mode.

VI. CONCLUSION

In this paper, the combination of geometric virtual structure and nonlinear line-of-sight guidance law is applied to multi-UAV formation. Through the numerical and semi-physical simulation, the practicality of the algorithm is verified. The main conclusions of this study are as follows:

1) After the formation UAVs receive the formation order from the ground, they simultaneously run the virtual formation. After each formation UAV tracks its own virtual leader, the formation is realized.
2) During flight, the longitudinal and lateral distance between each UAV and the virtual formation can maintain a set distance in the straight mode. In the arc mode, adjustments are made to the pitch angle to compensate for the height variation due to different radii. At the same time, it should be noted that various coupling factors can contribute to an increase in the bias of formation maintenance in the straight mode.
3) After conducting semi-physical simulations for four different formation shapes, the algorithm discussed in this paper exhibits excellent formation performance in straight mode. Due to the adjustments of speeds, biases during the arc mode increase but gradually converge. The results from four sets of experiments indicate that as long as the safety distance of the UAV is maintained, α_f and d_f have no significant impact on flight.

In the next step, we can refer to the formation transformation method proposed in literature [40] to address the problem of formation transformation in an environment with unknown obstacles.

CONFLICTS OF INTEREST

The authors declare no conflict of interest.

REFERENCES

[1] K. Qiu, C. Zhou, Y. Liu, L. Gao, X. Dong, and J. Cao, "Research on the development and application of unmanned aerial vehicles," in *Proc. 2nd Int. Conf. Artif. Intell. China (ChinaAI)*, Urumqi, China, Jul. 2019, pp. 523–530.

[2] L. Bai, Z. Zhao, X. Meng, Y. Wang, Q. Rao, and X. Deng, "Research on UAV formation simulation and evaluation technology," in *Proc. 5th Int. Conf. Intell. Auto. Syst. (ICoIAS)*, Dalian, China, Sep. 2022, pp. 166–171.
[3] W. Jianhong, R. A. Ramirez-Mendoza, and T. Xiaojun, "Target tracking algorithms for multi-UAVs formation cooperative detection," *Syst. Sci. Control Eng.*, vol. 9, no. 1, pp. 417–429, Jan. 2021, doi: 10.1080/21642583.2021.1916789.
[4] L. Cao, G.-P. Liu, and D.-W. Zhang, "A leader-follower formation strategy for networked multi-agent systems based on the PI predictive control method," in *Proc. 40th Chin. Control Conf. (CCC)*, Shanghai, China, Jul. 2021, pp. 4763–4768.
[5] J. Li, J. Liu, S. Huangfu, G. Cao, and D. Yu, "Leader-follower formation of light-weight UAVs with novel active disturbance rejection control," *Appl. Math. Model.*, vol. 117, pp. 577–591, May 2023, doi: 10.1016/j.apm.2022.12.032.
[6] X. Ai and J. Yu, "Flatness-based finite-time leader–follower formation control of multiple quadrotors with external disturbances," *Aerosp. Sci. Technol.*, vol. 92, pp. 20–33, Sep. 2019, doi: 10.1016/j.ast.2019.05.060.
[7] L. Yunhe, L. Bo, and N. Xiaowei, "Research on self-organizing behavior-based UAV formation based on distributed control," in *Proc. 3rd Int. Conf. Vis., Image Signal Process.*, Vancouver, BC, Canada, Aug. 2019, pp. 1–5.
[8] M. B. Emile, O. M. Shehata, and A. A. El-Badawy, "A decentralized control of multiple unmanned aerial vehicles formation flight considering obstacle avoidance," in *Proc. 8th Int. Conf. Control, Mechatronics Autom. (ICCMA)*, Moscow, Russia, Nov. 2020, pp. 68–73.
[9] L. Li, W. Sheng, and C. Hu, "Research on formation keeping of multi-rotor UAVs based on improved virtual structure method," in *Proc. 2nd Int. Conf. Artif. Intell. Comput. Sci.*, Zhejiang, China, Jul. 2020, Art. no. 012106.
[10] H. Su, X. Wang, and Z. Lin, "Flocking of multi-agents with a virtual leader," *IEEE Trans. Autom. Control*, vol. 54, no. 2, pp. 293–307, Feb. 2009, doi: 10.1109/tac.2008.2010897.
[11] Y. Duan, Z. Gao, Z. Peng, W. Yang, and Y. Wang, "Formation transformation based on leader-follower algorithm," *Int. J. Technol. Hum. Interact.*, vol. 15, no. 3, pp. 28–46, Jul. 2019, doi: 10.4018/ijthi.2019070103.
[12] Y. Jia and W. Zhang, "Three-dimensional leader-follower formation flocking of multi-agent system," in *Pro. Int. Conf. Artif. Life. Robot.*, Miyazaki, Japan, Jan. 2017, pp. 5–8.
[13] A. Naderolasli, K. Shojaei, and A. Chatraei, "Finite-time velocity-free adaptive neural constrained cooperative control of Euler–Lagrange systems," *Trans. Inst. Meas. Control*, to be published, doi: 10.1177/01423312231154625.
[14] M. Mahfouz, A. T. Hafez, M. M. Ashry, and G. Elnashar, "Cyclic leader-follower strategy for cooperative unmanned aerial vehicles," in *Proc. IEEE Int. Conf. Veh. Electron. Saf. (ICVES)*, Cairo, Egypt, Sep. 2019, pp. 1–6.
[15] C. Wang, J. Du, L. Ruan, J. Lv, and S. Tian, "Research on collision avoidance between UAV flocks using behavior-based approach," in *Proc. China. Satell. Navigat. Conf. (CSNC)*, Jiangxi, China, May 2021, pp. 356–365.
[16] G. Lee and D. Chwa, "Decentralized behavior-based formation control of multiple robots considering obstacle avoidance," *Intell. Service Robot.*, vol. 11, no. 1, pp. 127–138, Jan. 2018, doi: 10.1007/s11370-017-0240-y.
[17] D. Zhou, Z. Wang, and M. Schwager, "Agile coordination and assistive collision avoidance for quadrotor swarms using virtual structures," *IEEE Trans. Robot.*, vol. 34, no. 4, pp. 916–923, Aug. 2018, doi: 10.1109/TRO.2018.2857477.
[18] J. Zhang, J. Yan, P. Zhang, and B. Wang, "Study on the collision avoidance of UAV cooperative formation with improved artificial potential field," *J. Xi'an Jiaotong Univ.*, vol. 52, no. 11, pp. 112–119, 2018, doi: 10.7652/xjtuxb201811017.
[19] M. F. S. Rabelo, A. S. Brandão, and M. Sarcinelli-Filho, "Landing a UAV on static or moving platforms using a formation controller," *IEEE Syst. J.*, vol. 15, no. 1, pp. 37–45, Mar. 2021, doi: 10.1109/JSYST.2020.2975139.
[20] Y. Yang, X. Xiong, and Y. Yan, "UAV formation trajectory planning algorithms: A review," *Drones*, vol. 7, no. 1, p. 62, Jan. 2023, doi: 10.3390/drones7010062.
[21] H. S. Yahia and A. S. Mohammed, "Path planning optimization in unmanned aerial vehicles using meta-heuristic algorithms: A systematic review," *Environ. Monitor. Assessment*, vol. 195, no. 1, p. 30, Jan. 2023, doi: 10.1007/s10661-022-10590-y.
[22] X. Wang, H. Wang, H. Zhang, M. Wang, L. Wang, K. Cui, C. Lu, and Y. Ding, "A mini review on UAV mission planning," *J. Ind. Manage. Optim.*, vol. 19, no. 5, pp. 3362–3382, 2023, doi: 10.3934/jimo.2022089.
[23] J. Tang, H. Duan, and S. Lao, "Swarm intelligence algorithms for multiple unmanned aerial vehicles collaboration: A comprehensive review," *Artif. Intell. Rev.*, vol. 56, no. 5, pp. 4295–4327, 2022, doi: 10.1007/s10462-022-10281-7.
[24] D. Deng, M. Yun, and G. Jie, "Cooperative mission planning of multiple UAVs based on parallel GAPSO algorithm," *Electron. Opt. Control*, vol. 23, no. 11, pp. 18–22, 2016.
[25] L. Hu, B. Xi, G. Yi, and H. Zhao, "A multiple heterogeneous UAVs reconnaissance mission planning and re-planning algorithm," *J. Syst. Eng. Electron.*, vol. 33, no. 6, pp. 1190–1207, 2022.
[26] X. Yu, X. Gao, L. Wang, X. Wang, Y. Ding, C. Lu, and S. Zhang, "Cooperative multi-UAV task assignment in cross-regional joint operations considering ammunition inventory," *Drones*, vol. 6, no. 3, p. 77, Mar. 2022, doi: 10.3390/drones6030077.
[27] X. Gao, L. Wang, X. Yu, X. Su, Y. Ding, C. Lu, H. Peng, and X. Wang, "Conditional probability based multi-objective cooperative task assignment for heterogeneous UAVs," *Eng. Appl. Artif. Intell.*, vol. 123, Aug. 2023, Art. no. 106404, doi: 10.1016/j.engappai.2023.106404.
[28] X. Wang, B. Li, X. Su, H. Peng, L. Wang, C. Lu, and C. Wang, "Autonomous dispatch trajectory planning on flight deck: A search-resampling-optimization framework," *Eng. Appl. Artif. Intell.*, vol. 119, Mar. 2023, Art. no. 105792, doi: 10.1016/j.engappai.2022.105792.
[29] X. Li, L. Wang, H. Wang, L. Tao, and X. Wang, "A warm-started trajectory planner for fixed-wing unmanned aerial vehicle formation," *Appl. Math. Model.*, vol. 122, pp. 200–219, Oct. 2023, doi: 10.1016/j.apm.2023.05.035.
[30] Q.-Y. Chen, Y.-F. Lu, G.-W. Jia, Y. Li, B.-J. Zhu, and J.-C. Lin, "Path planning for UAVs formation reconfiguration based on Dubins trajectory," *J. Central South Univ.*, vol. 25, no. 11, pp. 2664–2676, Dec. 2018, doi: 10.1007/s11771-018-3944-z.
[31] X. Ge and Q.-L. Han, "Distributed formation control of networked multi-agent systems using a dynamic event-triggered communication mechanism," *IEEE Trans. Ind. Electron.*, vol. 64, no. 10, pp. 8118–8127, Oct. 2017, doi: 10.1109/TIE.2017.2701778.
[32] V. Walter, N. Staub, A. Franchi, and M. Saska, "UVDAR system for visual relative localization with application to leader–follower formations of multirotor UAVs," *IEEE Robot. Autom. Lett.*, vol. 4, no. 3, pp. 2637–2644, Jul. 2019, doi: 10.1109/LRA.2019.2901683.
[33] H. Liu, Y. Lyu, and W. Zhao, "Robust visual servoing formation tracking control for quadrotor UAV team," *Aerosp. Sci. Technol.*, vol. 106, Nov. 2020, Art. no. 106061, doi: 10.1016/j.ast.2020.106061.
[34] H. Li, T. Long, J. Sun, and G. Xu, "Adaptive line-of-sight method for 3D path following of UAVs," *Acta Aeronauticaet Astronautica Sinica*, vol. 43, no. 9, 2022, Art. no. 326105, doi: 10.7527/S1000-6893.2021.26105.
[35] J. Yang, A. G. Thomas, S. Singh, S. Baldi, and X. Wang, "A semi-physical platform for guidance and formations of fixed-wing unmanned aerial vehicles," *Sensors*, vol. 20, no. 4, p. 1136, Feb. 2020, doi: 10.3390/s20041136.
[36] S. Li, D. Zhao, J. Ye, and Q. Deng, "Design and realization of simulation TestBed for intelligent unmanned swarm system," in *Proc. 3rd Int. Conf. Comput. Inf. Big Data Appl.*, Hubei, China, Mar. 2022, pp. 1–6.
[37] C. Yan, X. Xiang, C. Wang, F. Li, X. Wang, X. Xu, and L. Shen, "Pascal: PopulAtion-specific curriculum-based MADRL for collision-free flocking with large-scale fixed-wing UAV swarms," *Aerosp. Sci. Technol.*, vol. 133, Feb. 2023, Art. no. 108091, doi: 10.1016/j.ast.2022.108091.
[38] M. M. Zhang, W. Ju, H. Q. Yun, Y. Liu, and Y. M. Liu, "Formation control method of multiple UAVs within considering collision avoidance," in *Proc. Int. Conf. Guid., Navigat. Control (ICGNC)*, Tianjin, China, Oct. 2020, pp. 5251–5263.
[39] Z. Shao, X. Zhu, Z. Zhou, B. Zhang, and Y. Wang, "Distributed formation keeping control of UAVs in 3-D dynamic environment," *Control Decis.*, vol. 31, no. 6, pp. 1065–1072, Jun. 2016, doi: 10.13195/j.kzyjc.2015.0462.
[40] Z. Cai, Y. Liu, J. Zhao, and Y. Wang, "Virtual structure and artificial potential field-based cooperative control for UAV formation," in *Proc. Int. Conf. Guid. Navigat. Control (ICGNC)*, Harbin, China, Aug. 2022, pp. 366–375.

JIANDONG GUO received the Ph.D. degree in aircraft design from the College of Aviation, Nanjing University of Aeronautics and Astronautics, Nanjing, China, in 2013. He is currently an Associate Research Fellow with the College of Automation Engineering and the Key Laboratory of Advanced Technology for Small and Medium-Sized UAV, Ministry of Industry and Information Technology, Nanjing University of Aeronautics and Astronautics. His current research interests mainly include advanced flight control law design and its multi-UAVs formation control.

ZHENGUANG LIU received the bachelor's degree from the College of Civil Aviation, Nanjing University of Aeronautics and Astronautics, in 2020, where he is currently pursuing the master's degree specializing in control engineering with the College of Automation Engineering. His research interests include formation control and intelligent algorithm.

YANGUO SONG received the Ph.D. degree in aircraft design from the Nanjing University of Aeronautics and Astronautics, China, in 2003. From May 2003 to May 2005, he was a Postdoctoral Fellow with the China Helicopter Research and Development Institute, China. In 2012, he was a Visiting Scholar with The Pennsylvania State University, State College, PA, USA. He is currently an Assistant Professor with the College of Aerospace Engineering, Nanjing University of Aeronautics and Astronautics, China. His primary research interests include aircraft design and flight mechanics and control.

CHANGFA YANG received the bachelor's degree in aircraft design and engineering from Northwestern Polytechnical University, Xi'an, China, in 2013. In 2022, he was the Deputy Director of the Equipment System Technology Research Department, Science and Technology Innovation Center, Jiangxi Aviation Research Institute. He has long been responsible for the overall plan for the development of advanced aviation weapons and equipment. He has one achievement and has authorized more than ten patents, such as invention/utility model/appearance. He undertook the completion of more than five models/pre-research projects, such as a certain type of immersive combat simulation training systems, a certain type of combat, training effectiveness simulation software, advanced business jet/bomber trainer, unmanned early warning aircraft, and tilting duct UAV design and technology research. His key technology demonstration and pre-research won the third-class individual merit of the Aviation Industry Group's pre-research (once).

CHENYU LIANG received the master's degree in control engineering from the Nanjing University of Aeronautics and Astronautics, Nanjing, China, in 2021. He is currently a Technical Researcher with Nanjing Changkong Technology, mainly engaged in the development of flight control embedded software. His primary research interests include advanced flight control algorithms and its semi-physical simulation.